

Investigation of the origin of neutrals in the main chamber of Alcator C-Mod

B. Lipschultz*, B. LaBombard, C.S. Pitcher, R. Boivin and J.L. Terry

*Massachusetts Institute of Technology Plasma Science & Fusion Center Cambridge Ma. 02139
U.S.A.*

Abstract: A series of experiments are described which are aimed at quantifying the relative contribution of divertor leakage and radial ion transport on neutral pressures surrounding the core plasma. Variations in the divertor geometry, magnetic equilibrium, divertor bypass leakage and confinement mode give evidence that cross-field transport competes with, or dominates, parallel transport in such a way that plasma exists far out in the Scrape-Off Layer (SOL) shadow and recycles on main chamber surfaces.

Based on a simple neutral flow model we estimate that neutrals escaping from leaks in the lower (closed) divertor during lower x-point operation contribute a smaller fraction (~10-30%) of the midplane pressure than main chamber recycling. The inferred leakage is much larger from the upper (open) divertor during upper x-point operation. Most neutrals escaping from either divertor do not directly travel to the midplane. Instead, they are redirected, most likely by ionization and/or collisions (elastic, charge exchange). We are able to infer toroidal and poloidal neutral attenuation lengths for this leakage of ~ 20 and ~50 cm respectively. Relatively high divertor pressures are found in upper-null (unbaffled) discharges. This suggests that the SOL plasma may take the place of the mechanical structure present in the lower divertor.

*E-mail address: Blip@psfc.mit.edu

1. Introduction

The Scrape-Off Layer (SOL) affects a number of aspects of tokamak operation. Plasma conditions outside the plasma core determine the characteristics of the divertor plasma and therefore the parallel power and particle flow profile at divertor or limiter surfaces. The resultant divertor impurity sources and helium compression in the divertor are also important. Moreover, the SOL can be very important for directly affecting the core - impurity sources in the main chamber, boundary conditions of density and temperature, and in particular, fueling and particle control.

There are two routes for neutrals to arrive in the region outside the core plasma, from which they may reach the core: 1) through radial ion transport to the main chamber surfaces with resultant recycling and creation of neutrals; and 2) by neutral leakage from the divertor (for a diverted plasma). In this paper we describe a series of experiments aimed at assessing the relative roles of these two paths for affecting the main chamber neutral pressure. These include variations in geometry, magnetic equilibrium, divertor bypass leakage and confinement mode.

Previous experiments concentrating on this subject imply that cross-field ion transport in Alcator C-Mod [1-5] can lead to large ion fluxes to main chamber surfaces and resultant neutral sources. A similar conclusion was reached for ASDEX-Upgrade [6]. This interpretation is suggested in part by the shape of the measured density profiles: Results from a number of experiments [7,8,6,9,10] have shown that the SOL can often be characterized by a region near the separatrix ('near' SOL) with a short density gradient length. Farther out in the SOL ('far' SOL), the density e-folding length can be much longer, giving the appearance of a 'shoulder'. The differences in gradients between the near and far SOL have been modeled as due to differences in radial ion transport [11,6,12,1,2,4] with cross field diffusion in the far SOL exceeding Bohm values. The difference between L- and H-mode plasmas is limited to a reduction in effective radial diffusivities in the near SOL [4].

It is reasonable to expect that the divertor geometry should play a role in neutral control [13,14]. Neutrals could leak from the divertor and directly travel to the midplane. Such non-local neutral sources have also been shown to give rise to a shoulder on the density profile [7,15]. The experimental results on this subject are varied, to say the least. Results from JET [16], JFT-2M [17], and DIII-D [18] indicate that increased divertor closure (geometry as well as closing leaks through the divertor structure) leads to a reduction in the midplane pressure. The most recent increase in geometrical closure of the JET divertor (while keeping the leakage the same) has increased the divertor pressure, without changing the midplane pressure [19]. An interpretation of this result is that the leaks through the divertor structure in JET no longer affect the midplane pressure [14]. Results from the closing of leaks on C-Mod and ASDEX-Upgrade lead to an increase in divertor pressure with no change in midplane pressure [10,20,21]. More specific

experiments were performed on C-Mod utilizing divertor bypass valves that could be used to change the leakage conductance even during a single discharge [13] [22]. These also implied little effect on the midplane pressure, even though the predicted leakage fluxes were many times the source due to gas fueling valves. A constant flux argument (flux independent of conductance) was invoked to explain this [13].

The question of the origin of midplane neutrals in a divertor tokamak raises other, more macroscopic issues. An important goal of the divertor configuration is to capture the power and particles leaving the core. In addition, the divertor concept is intended to remove the impurity source locations to surfaces far from the plasma core, ideally at divertor surfaces. A better understanding of the limits of the divertor configuration will allow us to make a more quantitative judgement between alternative particle and heat flux handling geometries.

The experiments reported here are aimed at better quantifying the relative contribution of divertor leakage and radial ion transport on the midplane pressure. By varying the location of limiters in the SOL we find that cross-field transport competes with, or dominates, parallel transport in such a way that plasma exists far out in the SOL shadow, thus leading to main chamber recycling. Changing the core transport from L- to H-mode leads to little or no effect on the far SOL indicating that the flux to the walls has not changed, just the gradients at the separatrix and the density in the core..

In an effort to assess the divertor leakage contribution to the midplane pressure we varied the lower closed divertor pressures (and by inference the leakage from the lower divertor) independent of core density. Based on a simple model we are able to estimate that the lower divertor contributes between ~10-30% of the midplane pressure, the rest supplied by main chamber recycling. In these experiments we also compared the lower closed divertor to the upper divertor which is completely open, without mechanical baffling. The more open upper divertor appears to create a high recycling condition similar to that of the much more closed lower divertor, leading to similar neutral pressures in either divertor. The leakage of neutrals from the upper open divertor to the midplane is much larger than from the lower divertor, and on a level comparable to main chamber recycling.

2. Experimental description

All results reported in this paper were obtained with deuterium discharges with $B \times \nabla B$ towards the bottom of the vessel. For most discharges the x-point was located at the bottom of the vessel where the closed, vertical plate divertor, is located (Fig. 1a). Unless otherwise specified all discharges are in D₂. Some experiments required the dominant x-point to be located at the top of the vessel where the divertor is completely open (Fig. 1a). The general characteristics and diagnostics of the Alcator C-Mod device can be found elsewhere. Further

details on some of the edge diagnostics have also been published previously [10,4]. Here we present some of the more relevant diagnostic descriptions.

The locations of the various pressure diagnostics are shown in Figures 1a-b. Baratron capacitance manometer gauges (~50 ms response time) are located in vertical ports connected to the upper and lower divertors as well as at the midplane of the torus in a large horizontal port. There are two such gauges in the lower divertor, one located at a port (herein called an ‘open’ port) with a diagnostic opening through which neutrals can escape back to the main chamber. The other is located at a port without a diagnostic opening (‘closed’ port where neutral leakage is minimal). Other gauges include a shielded Bayard-Alpert ionization gauge (response time ~ 30 ms), located at the outer midplane, and several Penning gauges (response time < 5 ms), located at several points toroidally (see Fig. 1b) and poloidally (Fig. 1a). All gauges are calibrated against the Baratron gauges. The Penning gauges have the additional constraint of requiring the full toroidal magnetic field on at the time of calibration. It is important to point out that the only diagnostic we have of the upper divertor is the Baratron gauge mentioned above.

The outer divertor bypass system [22] allows the neutral leakage through the closed lower divertor to the main chamber to be varied dynamically during a discharge. There are 10 discrete toroidally-spaced valves, the locations of which are shown in Fig. 1b.

High resolution profiles of electron temperature and density in the SOL are obtained from two scanning probe systems, both of which are shown in Fig. 1a: a vertical-scanning probe that samples plasma at a position ‘upstream’ from the entrance to the outer divertor, and a horizontally-scanning probe that records plasma conditions 10 cm above the midplane.

For the experiments described herein we vary the magnetic equilibrium from lower to upper x-point. The measure of the equilibrium variation is the radial gap between the first and second separatrix mapped to the outer midplane, denoted by the parameter SSEP in the EFIT equilibrium solver code [23]. SSEP is negative for lower x-point dominant, positive for the upper null. Typical minimum values are -15 to -20 mm for lower x-point equilibria, but often the magnitude of SSEP is larger.

3. Main chamber sources of neutrals

In the introduction we referred to two potential contributors to the neutral population surrounding the plasma (in general we are referring to the neutral density at the outer midplane): 1) ion fluxes recycling off of main chamber surfaces as neutrals; and 2) neutral leakage from the divertor. Note that the former forms a circuit of ions transported across the magnetic field, flowing out of the core and SOL, and returning to the core and SOL as neutrals. The latter forms a different circuit – ions leave the SOL by flowing along the field into the divertor, recycling as neutrals and reentering the core or SOL (leaking through divertor structure) where they are

ionized, closing the loop. In this section we will first discuss the evidence for the existence and magnitude of the first loop.

3.1 Main chamber neutrals due to cross-field ion flow

3.1.1 General characterization

We briefly review the characteristics of the SOL and the techniques used in this section. Figure 2 includes density (Fig. 2a) and temperature (Fig. 2b) profiles across the SOL for 9 different core densities $1 \times 10^{20} \text{ m}^{-3} \leq \bar{n}_e \leq 2.6 \times 10^{20} \text{ m}^{-3}$ ($0.17 \leq n_{\text{Greenwald}} \leq 0.45$), derived from the horizontal scanning probe. The distance from the separatrix is labeled ‘ ρ ’. The location of the limiter is indicated, varying from $\rho = 19\text{-}22 \text{ mm}$ for these data. The near SOL ($0.4 \text{ mm} \leq \rho$) has a short e-folding length that is similar to its width. The density at the limiter and in its shadow is strongly dependent on \bar{n}_e . At the two highest densities shown the density profile near the separatrix flattens as well.

The temperature near the separatrix varies little as one might expect from a region where parallel conduction dominates energy transport. Near the separatrix the temperature gradients vary little as \bar{n}_e is increased. The gradient scale length gradually increases as a function of ρ . In these measurements and other measurements in the region beyond the limiter, the temperature is almost always in the range 5-10 eV. Thus there is very little gradient in temperature profile beyond that point.

As the density is increased beyond the range shown here, the flat region of the density profile starts moving inside the separatrix. At the same time the separatrix temperature drops, indicative that parallel conduction is no longer determining the temperature there. The details of the evolution of SOL conditions as the density limit is approached can be found elsewhere [5].

In previous work [4] we have developed an interpretive analysis of probe and ionization source profiles to determine an effective cross-field diffusion coefficient, D_{eff} , and radial ion fluxes, $\Gamma_{\perp,i}$. The cross-field ion flux density entering the region between two poloidal limiters, $\Gamma_{\perp,\text{lim}}$ can be determined by integrating the parallel ion current incident on those limiters.

$$\int_{\text{lim. face}} \Gamma_{\perp,i} \cdot dA_{\perp} = \int_{\text{lim. sides}} \Gamma_{\parallel,i} \cdot dA_{\parallel} + \int_{\text{between limiters}} S_i \cdot dV \quad (1)$$

The assumption underlying the use of this continuity equation is that ionization in the limiter shadow must be small compared to parallel flux term in the continuity equation:

$$\int_{\text{lim. sides}} \Gamma_{i,\parallel} \cdot dA_{\parallel} \gg \int_{\text{between limiters}} S_i \cdot dV, \text{ or} \quad (2)$$

$$2nc_s / L \gg S_i$$

Where L is the toroidal spacing, S_i is the ionization rate density, and c_s is the ion sound speed. For the region between two limiters where the horizontal scanning probe is inserted this criterion is easily satisfied. Typical values of the parameters are $n_e \sim 1 \times 10^{19} \text{ m}^{-3}$, $T_e \sim 10 \text{ eV}$, $L \sim 0.8 \text{ m}$, and $S_i \sim 2 \times 10^{22} \text{ m}^{-3} \text{ s}^{-1}$. $\Gamma_{\perp, \text{lim}}$, shown in Figure 2c, scales linearly with the midplane pressure (which itself scales as $\sim \bar{n}_e^4$ [3,4]). The top horizontal axis shows an estimate of the inward flux of neutrals, $\Gamma_{\perp, 0}$, based on the midplane pressure. We see that radially outward ion fluxes are balanced by the inward neutral fluxes to within a reasonable factor (~ 2). It should be pointed out that a previously reported set of data taken over a wider variety of plasma currents and limiter gaps showed a departure from a linear relationship between fluxes to the limiter and midplane neutral pressures at the highest densities [4]. Therefore there may be some concern that the measurements at the outer midplane might be somehow unusual, and in particular high, compared to other poloidal locations. But we have found that the neutral pressures (and perhaps radial ion fluxes) at the outer midplane are lower than at other locations poloidally around the plasma, but outside the divertor. For example, pressures at the top of the vessel can be 2-10x that at the midplane. In addition, D_{α} measurements show that at times recycling at the inner wall can be higher than at the outer midplane. Furthermore, flux surfaces in the far SOL impact on the horizontal baffle section of the outer divertor leading to additional plasma recycling outside the lower divertor proper.

3.1.2 Effect of changes in core confinement

The characteristics of the far SOL appear to be relatively unaffected by the transition from L- to H-mode. In figure 3 we show the effects on the SOL of a transition from L- to H-mode. The H-mode density profile (Fig. 3a) is from a time ~ 140 msec after the transition when the core density is close to its H-mode level of $2.6 \times 10^{20} \text{ m}^{-3}$ (from $1.6 \times 10^{20} \text{ m}^{-3}$ in L-mode). The far SOL is unaffected by the change in core confinement even though the line-averaged density, \bar{n}_e , nearly doubles. In the near SOL region the electron pressure and density as well as their gradients are larger. The electron temperature is slightly lower in this region, leading to an increased collisionality. Utilizing these profiles and the local $\text{Ly}\alpha$ emissivity [24], a local effective particle diffusivity, $D_{\text{eff}} \equiv \Gamma_{\perp, i} / \nabla n_e$ just outside the separatrix is obtained [4,5] (Fig. 3b). After the transition to H-mode D_{eff} drops by about a factor of 2-3. However, the effective particle diffusivity in the far SOL is essentially unchanged at levels of $0.5 \text{ m}^2/\text{sec}$, several times Bohm. One can also compute the average radial transport velocity associated with the radial ion flux, $v_{\perp} \equiv \Gamma_{\perp, i} / n_e$. This is shown in Fig. 3c. Because density is decreasing throughout the SOL, v_{\perp} increases across the SOL ($v_{\perp, \text{min}}$ in Fig. 3d is discussed later in Section 4.1). The radial outward velocity is reduced in H-mode in the near SOL. We note that the velocities determined

by such an analysis are lower than that found through analysis of fluctuation transport by probes[25] and D_{α} emission [26].

The correlation between plasma density, flux and neutral pressure at the limiter extends to H-mode plasmas. In Fig. 4 we provide, for both L-mode and H-mode plasmas, the scaling of density (Fig. 4a) and radial ion flux at the limiter radius (Fig. 4b) as well as the midplane pressure (Fig. 4c) vs. the core line-averaged density. All measures scale similarly. The L- and H-mode data points are often from the same discharge, before and after the transition. The H-mode data appears to have a similar trend as the L-mode data, but displaced to higher core densities. Thus, like Figure 3, the change from L- to H-mode leaves the radial ion fluxes and resultant main chamber recycling the same. On the other hand the lack of variation of the midplane pressure from L- to H-mode might also be consistent with neutral leakage affecting the midplane pressure: Divertor pressures (and the accompanying leakage) also do not change significantly in the transition.

3.1.3 Effect of changes in the limiter gap

One method used to explore the strength of radial transport is to radially shift the separatrix of a diverted equilibrium until it is coincident with a main chamber surface. The magnetic equilibrium including lower x-point, separatrix, and divertor strike points are retained. Figure 5 shows the density profiles at the outer SOL midplane (horizontally-scanning probe located toroidally between two poloidal limiters - Fig. 1b) for four ohmic discharges with very similar core density ($1.5 \times 10^{20} \text{ m}^{-3}$) and plasma current (800 kA) where the inner gap (separatrix to inner wall) was varied from 0 to 15 mm. The gap between the separatrix and the outer limiters was kept large (12-25 mm). The flux surface corresponding to a 12 mm gap at the outside edge is equivalent to a gap of 15 mm when followed to the inner edge. We find that the SOL characteristics, including not only density and temperature, but also the midplane pressure, are relatively unaffected by the flux surfaces (0-15 mm) being intercepted by the inner wall, 'filling-in' around it. This is certainly consistent with a model with strong radial transport. Alternatively, the insertion of a limiter leads to recycling in just the right way that the recycled neutrals are ionized and give the same density profile as without a limiter. This would still require that power be transported into the shadow of the limiter, sufficient to ionize those neutrals. In any case limiting the plasma on the inner wall does not lower the density in the shadowed region and the ion fluxes to the first wall surfaces (with resultant production of neutrals) further out in the SOL remains the same.

Similar experiments were carried out by limiting the plasma on the outer limiter, while keeping the inner gap constant. The results are more confused for this case. Again, there is a filling-in effect such that the vertical scanning probe sees little effect on the far SOL. The

amount of recycling light in the shadow of the limiter (and ion flux into the limiter shadow) rises significantly, but the midplane pressure hardly changes. It is somewhat surprising that the introduction of such a strong localized recycling source does not lead to significant changes in the midplane pressure at a nearby toroidal location. Experiments described later in this paper indicate that such localized neutral sources are smoothed out by neutral transport in the toroidal and poloidal directions.

3.2 Main chamber neutrals due to divertor neutral leakage

At issue is the level of neutral leakage out of the divertor, and whether such neutrals reach the midplane and the pressure measurement gauge. We do not directly measure the flow, rather we measure pressures and try to infer the flow magnitude relative to main chamber recycling.

3.2.1 General observations: lower x-point discharges

The strongest argument that neutrals are leaking out of the divertor and directly reaching the midplane measurement gauge is the correlation between the pressures measured in the divertor and at the midplane [27]. In Figure 6 we present the scaling of midplane pressure against the pressure measured at three divertor locations (see Figures 1a-b): a) the lower divertor at a closed port (Fig. 6a); b) the lower divertor at an open port (Fig. 6b); and c) the upper divertor (Fig. 6c, this divertor is very open because there is no mechanical baffling). The data are from two days of experiments where the density was varied in ohmic, lower single-null discharges while the gaps and plasma current (0.8 MA) were held constant. Attached and detached discharges are included. Both the lower open port divertor and upper divertor pressures correlate linearly with the midplane pressure, the scalings of the two pressures roughly a factor of 9 apart. The correlation is poorer for the lower divertor (closed port) pressure. Neutrals leak out of the lower divertor mainly through the five diagnostic openings in the outer divertor, one of which has the ‘open port divertor gauge’ located in it. Thus that gauge should be proportional to the leakage flux. The neutrals that collect below closed divertor sections must travel toroidally to reach the diagnostic openings in the outer divertor before escaping the divertor towards the midplane. The difference between lower divertor open and closed port pressures and their respective scalings could possibly be due to variations in that toroidal transport, perhaps dependent on transport regime (e.g. detached vs. attached).

The linear scaling between the lower divertor (open port) pressure (P_{LD}) and the midplane pressure ($P_{0,Mid}$) is consistent with a simple model which balances the number of neutrals entering the core plasma per unit time ($\Gamma_{\perp,0}$) across the separatrix at the outer edge (area, A_{Plasma}) with the neutral flux through a divertor leakage area, $A_{L,Leak}$ [27]:

$$\Gamma_{\perp,0} \equiv \beta P_{0,Mid} A_{Plasma} \approx f \cdot \beta \cdot (P_{LD} A_{L,Leak}) \quad (3)$$

We have assumed some effective transmission factor f , for neutrals to directly stream from the divertor to the midplane. We expect f to be less than 1. The conversion factor, β , is from the proportionality between pressure and flux in the case of free molecular flow, $\beta \cdot P = n\bar{c} / 4$, where $\beta = 1.14 \times 10^{22}$ D atoms/m³/mTorr for room temperature D₂ molecules. Implicit in Eq. 3 is the assumption that the measured midplane pressure is representative of a toroidal and poloidal average of neutral pressures over the area A_{Plasma} . β drops out and the result is the relationship

$$P_{0,Mid} \approx f(P_{LD} R_A) \quad (4)$$

where the ratio of $A_{L,Leak}$ to A_{Plasma} , $R_A = .0136$. On the basis of this scaling and Fig. 6b, where $f R_A = .033$, we obtain a value $f \sim 2.5$. This obviously large number could be due to the simplicity of the model, an underestimate of $A_{L,Leak}$, and/or, as we will see, lack of inclusion of other effects.

It is somewhat puzzling to observe a similar linear dependence of the midplane pressure on the upper divertor pressure if the lower divertor is the dominant source of leakage. The area of the opening through which neutrals escape the upper divertor towards the midplane is ~ 4800 cm², roughly 8x that of the total lower divertor diagnostic openings. We can expand Eq. 4 to include leakage from the upper divertor:

$$P_{0,Mid} \approx f(P_{UD} R_{UA} + P_{LD} R_{LA}) \quad (5)$$

where we have defined separate constants, R_A , for the two divertors and assumed that the transmission of neutrals from a leakage aperture to the midplane is the same for upper and lower divertors. The latter is reasonable given that the leakage locations are symmetric about the midplane and that the outer edge of the plasma is fairly symmetric as well. Because $P_{UD} \sim P_{LD}/9$ (Fig. 6bc) and $R_{UA} \sim 8 R_{LA}$ we expect the contribution to the midplane pressure from the two divertors to be nearly the same based on the measured pressures. So, if the lower divertor is making a contribution to the midplane pressure during lower single-null discharges, the upper divertor is likely making a contribution of similar magnitude. Based on Eq. 5, the value of the transmission factor, f , drops to more a reasonable value, 1.25, but still too high. On the other hand, there is still a clear inconsistency in the physics model. Where are the ions coming from that produce such a large source of neutrals in the upper divertor if, for lower x-point discharges, most of the open field lines of the SOL terminate on the lower divertor? It could only be due to recycling in the main chamber somewhere, perhaps at the inner wall, or field lines on flux

surfaces beyond the second separatrix and limiter, even farther out in the SOL hitting vessel surfaces at the top of the vessel (The upper x-point is outside the vessel for most of these data points). In either case radial transport must be moving ions across the field at a significant level to populate those flux surfaces. This points out that we should generalize Eq. 5 to include the contribution to the midplane pressure from main chamber recycling (not from the upper divertor), P_{MCR} :

$$P_{0,Mid} \approx f(P_{UD}R_{UA} + P_{LD}R_{LA}) + P_{MCR} \quad (6)$$

Again, using a reasonable value for f (0.5) we can ask what the contribution of P_{MCR} is to $P_{0,Mid}$. Substituting in the scaling relationships of Fig. 6bc between P_{UD} , P_{LD} and $P_{0,Mid}$ we find $P_{MCR} \sim 0.67 \times P_{0,Mid}$. Since in reality the upper divertor is just part of the main chamber (lower x-point at the bottom) then inclusion of its contribution to the midplane pressure in P_{MCR} implies that main chamber recycling contributes 80% of the midplane pressure. Now clearly the simplicity of this model may allow for considerable change in this result, perhaps even reversing the numbers such that divertor leakage completely dominates the midplane pressure. We will attempt in the remainder of the paper to estimate the contributions of divertor leakage and main chamber recycling on the midplane pressure from different sets of data.

To give the reader some appreciation of the fluxes being discussed, we review the throughputs of such leaks. We assume that the amount of leakage is predicted by simple free molecular flow through an aperture. Given the area of the lower divertor openings, the conductance ($\sim 20 \text{ m}^3/\text{sec}$) and driving pressure lead to leakage fluxes in the range $0.5\text{-}2 \times 10^{22}$ particle/sec for typical lower open divertor conditions (5-20 mTorr). This neutral leak rate is of similar magnitude as the integrated ion flux to the lower outer divertor plate, and $\sim 20\times$ that used to maintain the plasma density through the torus gas-puff valves! It would seem that at these values of leakage the gas-puff valve would be ineffective for density control relative to changes in divertor geometry and x-point location. But it is not.

3.2.2 Effect of changes in inner limiter gap

Because the divertor and midplane pressures are so strongly correlated with each other and with the core plasma line-averaged density we have attempted to find ways of varying the divertor pressure, and thus the source of neutral leakage, independent of \bar{n}_e . Several methods were developed for this purpose. Such an effect occurred in the experiments where the plasma was limited on the inner wall. Shown in Figure 7 are data from the 4 shots shown in Fig. 5, with 3 time points per shot. The lower (closed) divertor pressure (Fig. 7a) is reduced by reduced power flow into the divertor as the plasma becomes limited. But the midplane pressure (Fig. 7b)

is relatively unaffected. The lower (open) port pressure measurement was not working for this run, but in general, its pressure is 2-3 x lower (we will use 2.5) than the closed port for such attached discharges. This data supplies us with a way of estimating the contribution of divertor leakage to the midplane pressure independent of main chamber contributions. We use the profiles of Fig. 5 and core conditions to select time slices from with $P_{MCR} \sim$ constant from limited to not-limited. The upper divertor pressure stays extremely low (~ 0.1 mTorr) and can be neglected. So we can solve for the change in midplane pressure, $\Delta P_{0, Mid}$, in going from limited to non-limited shots. Using Eq. 6, the terms from P_{MCR} and P_{UD} drop out:

$$\Delta P_{0, Mid} = \alpha \cdot \Delta P_{LD} \quad (7)$$

where $\alpha = f \cdot R_{LA}$). We obtain $\alpha = .005-.0010$, $f = .33-.72$ and the fraction of $P_{0, Mid}$ due to main chamber recycling, $P_{MCR}/P_{0, Mid}$, is $\sim 74-87\%$.

We note that this estimation of $P_{MCR}/P_{0, Mid}$, and those following, are not dependent on knowing the values of f and R_{LA} . They are absorbed into one fit parameter, α , which is then used to determine $P_{MCR} = P_{0, Mid} - \alpha \cdot (P_{LD} + 8 \cdot P_{UD})$. The factor of 8 is the ratio of upper to lower leakage aperture areas.

3.2.3 Effect of changes in up-down divertor balance

A second method of varying the divertor pressure independent of the core is to vary the equilibrium from single-null x-point at the lower divertor to double-null (symmetric up-down x-points). We track the variation in equilibrium using SSEP. Shown in Figure 8 are the upper divertor, midplane and lower divertor (closed and open ports) pressures vs. SSEP, where SSEP=0 denotes a double-null and negative values of SSEP correspond to the lower x-point being dominant. The lower divertor pressure at an open port was typically $\sim 40\%$ that of the lower, closed divertor pressure for these attached discharges. When SSEP is a large negative value the lower divertor pressures are much higher than that at the upper divertor. At the other extreme, when the equilibrium is double-null, the two divertor pressures are closer. Ignoring outlier points, the midplane pressure may be considered to increase slightly as SSEP approaches 0.

The variations in pressure as a function of SSEP shown in Figure 8 provide a test for any model of leakage. We can again utilize Eq. 6 (or 7) to estimate the various contributions to the midplane pressure as SSEP changes, similar to what was done for the data of Fig. 7. We again assume that since the core plasma parameters are being held constant, that the term due to P_{MCR} is held constant. Consequently, we find a value of α (and f) that fits the data, and solve for P_{MCR} . The curves in Fig. 8 show the result of fitting the pressure data from the divertors and the

model prediction of the midplane pressure with the derived value of $\alpha = .002$ ($f \sim 12.5\%$). The contribution of main chamber recycling to the midplane pressure, $P_{MCR} \sim 0.27$ mTorr ($P_{MCR}/P_{0,Mid} \sim 0.9$). The gas valve puff rate was very low (actually off for the H-mode data) compared to the fluxes involved here, ~ 20 Torr-l/sec (1.2×10^{21} /sec) equivalent to 0.015 mTorr contribution to the midplane pressure. The contribution of leakage out of the lower divertor is also small, $\leq 10\%$ of $P_{0,Mid}$.

3.2.4 Evolution of upper x-point discharge

Based on the results shown in Figure 8 discharges were programmed to take SSEP beyond 0 to achieve upper single-null dominant equilibria. Two discharges are shown in Figure 9, one with SSEP (Fig. 9a) varied from -15 mm to $+8$ mm, the other with little SSEP variation for reference. In addition, for these experiments, several Penning gauges were available, at locations along the outer wall as shown in Figure 1. The plasma is formed limited on the inner wall, becoming diverted at ~ 0.25 seconds. The density reaches an equilibrium value of $0.95 \times 10^{20} \text{ m}^{-3}$ at 0.5 seconds, held constant thereafter by density feedback to the gas feed valve. As the magnetic equilibrium becomes double-null (SSEP=0), the upper (Fig. 9b) and lower divertor (closed, Fig. 9f) pressures reach similar values as seen in Figure 7. In addition, we find that the outer wall pressures (Fig. 9c-e) at the three poloidal locations appear to equalize as well, but at lower values than either the upper or lower divertors. As SSEP is increased still further, to a dominant upper x-point, the upper divertor and outer wall (upper) pressures continue to increase strongly. The midplane pressure increases by almost a factor of 2. Again, variation in the lower divertor pressure has little effect on the midplane pressure. The lack of changes in the outer wall (lower) pressure which is closest to the lower divertor could be due to its distance from an open port (~ 18 degrees toroidally) or that its pressure is dominated by other sources (e.g. main chamber recycling or leakage from the upper divertor). At the highest upper divertor pressures there are signs of leakage from that divertor affecting the outer wall (upper) pressure and that at the midplane.

We can apply the same neutral flux balance model given above (Eq. 6 or 7) to the data of Figure 9. The same values of α ($\sim .002$) & f ($\sim 12\%$), give a good fit to the time variation in outer wall (midplane) pressure due to neutral leakage out of the divertors. The resultant value of P_{MCR} increases ($\sim .45$ mTorr, $\sim 0.9 \times P_{0,Mid}$) compared to the data of Fig. 7 to reflect the difference in main chamber recycling. The lower divertor contribution to the midplane pressure is again small ($\leq 10\%$ of P_{MCR}), even for the highest lower divertor pressures shown in Figure 9. The upper divertor leakage contribution rises to $\sim 0.7-1.0 \times P_{MCR}$ as the upper divertor pressure rises.

3.2.5 Effect of toroidal variation in leakage

The above experiments make changes in divertor leakage that are essentially toroidally uniform in nature. The pressure gauges are located at specific toroidal points (Fig. 1b). Utilizing the 10 toroidally equi-spaced divertor bypass valves we further explore the effect of divertor leakage. Figure 10 shows the result of one discharge where the divertor bypass valves from three toroidally-adjacent bypass locations (at -18° , 18° , 54° , Fig. 1b) were opened and closed with period 200 ms during plasma discharges. The bypass valves are located 126° and 90° toroidally from the midplane and upper divertor gauges respectively. One of the valves (-18 degrees) was at the same toroidal location as the Penning gauges. The lower divertor (closed) gauge was located toroidally between two valves (18° and 54°). The plasma current is held constant and \bar{n}_e (Fig. 10a) is increasing. Helium was utilized as the fuel gas for these experiments to eliminate the uncertainty of the role of the wall as a reservoir for neutrals. The bypass valve state does correlate with changes in all gauges (Fig. 10c-f) as well as \bar{n}_e . During the period that the bypass valves are opening or closing (~ 20 ms, shaded regions, Fig. 10b), there is a prompt effect on the outer wall (lower) Penning gauge (Fig. 10e). We attribute this to neutrals directly reaching the gauge from the nearby bypass valves. The midplane gauges, the divertor gauges and \bar{n}_e show similar, slower, changes indicative of neutrals being converted to ions before recycling elsewhere around the torus. The small change in the outer wall (upper) gauge, under close examination, potentially exhibits some of the same prompt effect as the outer wall (lower) gauge but the effect is very small.

An important aspect of the data shown above is that one of the bypass valves is located at the same toroidal location as the outer wall Penning gauges. We also varied the location of the three adjacent valves from near to the Penning gauges to far from them. Figure 11a-b shows the effect on \bar{n}_e and the Outer wall (lower) gauge for one valve cycle, including the case from Figure 10 (shown as a solid line) as well as a case where the closest of the three valves was 72 degrees away from the outer wall gauge (dashed line). When the bypass valves are farther away from the gauge, the prompt effect on the outer wall (lower) gauge disappears and its change in pressure is smaller relative to the increase in density. The results of varying the toroidal locations of valves to still more locations is summarized in Figures 11c-d. The change in pressure measured at the outer wall lower (11c) and midplane (11d) gauges are plotted against the change in density caused by the release of gas. The data are grouped by cases where the valves are located just by the gauge (triangles) and for valves located 72 - 108 degrees away (circles). These results indicate that only the region of the outer wall poloidally and toroidally near the outer divertor valve is affected directly by neutral leakage. In addition, $\sim 50\%$ of the pressure rise on the outer wall gauge near the bypass valves is due to a toroidally uniform rise. We find ~ 20 degree e-folding distance toroidally (~ 20 cm) for the prompt effect. The decay length poloidally is difficult to

estimate but based on the change in outer wall (upper, Fig. 11c) gauge relative to that of the outer wall (lower, Fig. 11e), it appears to be of order 40-50 cm. Thus, neutrals leaking from the divertor are converted to ions, travel around the torus and recycle in the main chamber near other gauges. This would explain the correlation of the slow time behavior between the gauges and the core \bar{n}_e . There are several possible reasons for the apparent attenuation of neutrals trying to travel toroidally and poloidally around the plasma: 1) interaction of released neutrals with the plasma in the SOL; 2) differences in location between outer wall midplane (in a large port volume) and lower gauges (directly on the outer wall); and 3) differences in response time between the outer wall gauges at the midplane (~ 20 ms) and below the midplane (< 5 ms).

4. Discussion

4.1 Main chamber neutrals due to cross-field transport

There is substantial evidence that radial ion fluxes are significant in causing plasma interaction with the main chamber surfaces in C-Mod. The inferred radial ion fluxes are generally consistent in scaling and magnitude with measured midplane neutral pressures and ionization sources [1,4]. The observed strong recycling (pressures and ionization light) at other points poloidally would indicate that the midplane analysis is not an anomaly and that neutrals are not just coming from the lower, or primary, divertor. In fact, it appears that recycling may be stronger at points even farther from the lower divertor than the midplane.

There is other supporting evidence for radial ion fluxes. Nachtrieb found that the concentrations of He⁺¹ and He⁺² in far SOL of C-Mod were roughly equal [28]. The electron temperature and density at the measurement probe were too low to account for ionization of helium in the local flux tube, therefore the helium is ionized in a hotter region of the edge plasma and is transported outward. A simple one-dimensional radial transport model reproduced the observed values of charge state flux and density, but only if rapid cross-field transport was included, increasing with distance from the separatrix. A constant cross-field diffusion coefficient of order 2 m²/s and an outward convection velocity profile increasing to of order 100 m/s in the far scrape-off layer is implied.

Far SOL transport and interaction with main chamber surfaces are not affected by the transition from L- to H-mode. The effects are limited to the core and the near SOL. Since the cross-field ion flux does not significantly change, the core density rises to be consistent with reduced cross-field gradient lengths.

Strong radial ion fluxes would also be consistent with the results of limiting the plasma on the inner wall (Fig. 5). The density in the outer midplane SOL (near and far) stays the same or increases as the inner gap is reduced to zero. The cross-field ion transport could be competing with parallel transport such that the effect of local obstacles is not communicated along field

lines very far. One way to quantify the ‘strength’ of radial, compared to parallel, transport is to determine a $v_{\perp,\min}$ needed for the ion flux crossing a given flux surface, $\Gamma_{\perp,i}$, to be equal to the integral of the parallel ion flux flowing to the divertor from that flux surface on outwards:

$$\Gamma_{\perp,i} = n v_{\perp,\min} 2\pi R L_{pol} \sim n M c_s \frac{B_{pol}}{B_{Tor}} 2\pi R \lambda_{\perp}, \quad (8)$$

$$v_{\perp,\min} \sim M c_s \lambda_{\perp} / L$$

We have approximated the integral of parallel fluxes by $2\pi R \lambda_{\perp}$. Assuming for the moment a Mach number, M , of 1, then in Figure 3d $v_{\perp,\min}$ can be compared to the $v_{\perp,i}$ (Fig. 3c) obtained from the continuity analysis. We see that the two profiles are very similar in magnitude and shape such that the radial velocity is high enough to compete with Mach 1 flow. If, as experimental data from the vertical scanning probe at the entrance of the divertor has shown [4], that flow is more in the range of $M=0.1$, then radial fluxes are more likely to be dominant.

We believe that the strong radial transport in the far SOL is convective in nature. Figure 2a-b illustrates the minimal gradients in the far SOL. T_e is roughly constant in the 5-10 eV range beyond the limiter. The density profile in the far SOL can be fairly flat at the higher densities as well. Thus, in regions lacking gradients in density (far SOL) or T_e (shadow of a limiter) power is being transported across the magnetic field, enough to sustain the plasma there against parallel conduction as well as the cost of ionizing neutrals. That is evidence of convected power.

An indirect effect of main chamber recycling is that impurity sources are created on surfaces close to the plasma core. Such impurity sources have a higher probability of reaching the plasma core than impurities originating in the divertor [29,30]. Better determination of the locations of main chamber recycling and impurity sources are needed.

4.2 Main chamber neutrals due to neutral leakage

A simple model, embodied in Eq. 6, was applied to a wide variety of data. The results were fairly consistent in the determination that main chamber recycling is the main contributor to the midplane pressure. Values of the fraction of the midplane pressure supplied by main chamber recycling range from 70 – 90%. Based on our limited data set we cannot determine if the variation in relative contributions of leakage and main chamber recycling to the midplane pressure is significantly dependent on plasma conditions.

We are naturally cautious of putting too much credence in the results of applying the simple flux balance model (Eq. 6 and 7). However, even simpler arguments imply that the results of its application are reasonable. For example, let us return to the data of Fig. 6. For lower-null discharges the pressure in the upper divertor is really just another wall pressure measurement,

but located at the top of the vessel. The data indicates that the pressure in that region is higher than at the midplane. So, since we know that this pressure is not due to lower divertor leakage it is apparent that main chamber recycling can generate neutral pressures in excess of that at the midplane. Furthermore, the contribution to the midplane pressure from the lower divertor leakage and transmission from the upper vessel appear of similar magnitude. Thus, any additional recycling at the outer half of the vessel will just increase the contribution of main chamber recycling to the midplane pressure above the maximum leakage from the lower divertor.

We can find further guidance on the validity of the results of applying Eq. 6 and 7 by revisiting the data of Fig. 7. This time let us assume that there is no main chamber recycling when the plasma is diverted. Then, we see when the separatrix is shifted against the inner wall, that the divertor pressure (and leakage) drops by about a factor of four. The midplane pressure is essentially unchanged (some cases it drops slightly, others it rises) implying that main chamber recycling must change from nothing to $P_{MCR}/P_{0, Mid} \sim 0.75$! This implies that main chamber recycling must exist and probably at levels approaching $P_{MCR}/P_{0, Mid} \sim 0.75$.

One possible problem inherent in these studies is that the divertor pressure gauges are somehow not indicative of the pressure in the divertor region. The divertor gauges are located outside the vessel in a vertical port. If, perhaps because of the proximity to where the neutrals are generated, the neutral temperature in the region behind the divertor plates is significantly higher than that at the pressure gauge, the predicted fluxes would be too high by $(T_{hot}/T_{cold})^{1/2}$. We have evidence that this effect is not large. An ionization gauge was located in a region fairly close to the leakage aperture, in the lower divertor open port, for several run periods. It registered the same ratio of open port to close port pressure as we currently observe with a pressure gauge much farther away, down the open port [31].

Another possible concern is that there is some reduction in leakage conductance from its free molecular value. This could be due to ionization, charge-exchange or elastic scattering interactions (We note that ionization would not provide a mechanism to enhance the pressure. It can only reduce the flux). But in this case these interactions would occur in the region between where the neutrals are generated and where they escape into the SOL. For example, at both the upper and lower divertors, the port (where the gauge is) is connected to the leakage aperture by a square cross-section 'pipe' of length ~ 25 cm. Three of the 4 sides of the pipe are metal (2 sides being the gussets described in Fig. 1. The third is the wall of the vessel), with the fourth side being dense plasma (when that divertor is being utilized). Neutral-plasma interactions are allowed along one side of that 'pipe' thus possibly reducing the neutral flux along its length.

There are other reasons to suspect that the conductances based on free molecular flow are too large. As estimated earlier in this paper, the total leakage out of the open lower divertor ports

is of the same order as the ion flux to the outer divertor plate. Since any such leaked neutral must return to the plate this implies that ion flux back into the throat of the divertor would be of similar magnitude as the ion flux to the outer divertor. Based on SOL profiles of n_e and T_e , such high ion fluxes would require parallel flow Mach numbers of ~ 0.5 [27]. This is not observed by the vertical scanning probe above the outer divertor plate, near the entrance to the divertor ($M \sim 0.1$). One way to make these observations consistent is if the loop formed by escaping neutrals being ionized and returning to the divertor is closer to the divertor than the probe. This would mean that neutrals are not making it to the midplane. A second possibility is, as described above, that the flux is being reduced due to neutral-plasma interactions on the way to the aperture. Any reduction in conductance would show up in Eq. 6 as a reduction in transmission, f .

The same concern about the magnitude of leakage flows is even more important for the upper divertor. There the free molecular flow conductance is 8x higher, and for the maximum pressures we have measured there, correspond to neutral fluxes that are 2-4 x higher than the total ion flux to the lower divertor. It is possible that the ion fluxes to the upper divertor are much larger than that arriving at the lower divertor (We do not measure the ion flux to the upper divertor plates). But we think that unlikely. Rather, as stated above, the effective conductance out of the divertor is probably smaller than that predicted by free molecular flow. Any such conclusion would apply to both the bottom and top divertors because of similar conductance geometries.

In the analyses using flux balance model (Eq. 6 and 7) we tended to treat the parameter, f , as an interim quantity, not as a physical quantity worth much attention. f was described as the probability of a free-streaming neutral reaching the midplane after escaping from a divertor. Values of f ranged from 0.1 – 0.72. In reality f probably includes other effects such as the validity of either using free-streaming molecular flow for conductance or the gauge pressures as discussed above. On the other hand, a second set of experiments, where the toroidal location of the divertor bypass valves were varied, allowed us to estimate the toroidal and poloidal attenuation of neutrals released from the lower divertor. If the poloidal attenuation lengths are really of order the distance from the divertor to the midplane then we would expect values of f near $1/e$, a value in the middle of the flux balance predictions of transmission probability.

The achievement of pressures in the upper divertor approaching that of the lower divertor is surprising. But if 90% of the leaked neutrals don't reach the midplane then it is likely that they are ionized and return to the divertor, leading to a high-recycling condition even in the open upper divertor. The SOL plasma outside the upper divertor takes the place of the mechanically closed structure of the lower divertor. The attenuation process requires in-depth neutral and plasma modelling.

Are there advantages to using a closed vs. open divertor? Both the open and closed divertors contain neutrals well enough to sustain similar neutral pressures. The primary advantage of the lower divertor in this area is that its effect on the midplane pressure is even smaller compared to the background level of main chamber recycling. There are, of course, other advantages to using a closed divertor. These have to do with a larger plasma surface contact area reducing the peak heat flux and forcing the initial trajectory of impurity neutrals to point away from the core. The advantages of a divertor over the limiter configuration with respect to neutrals may have been compromised by both leaks and by recycling in the main chamber. Better understanding of and ability to predict radial transport will allow the ability to predict the performance of future divertor designs.

It is not clear how applicable these results are to other variations in divertor geometry. Our primary concern is that the location of the divertor leakage pathway may be very important in determining its effect. For example, the closer the leakage outlet is to the midplane and the farther it is from the SOL plasma, the larger effect it will have.

6. Summary

The results of a series of experiments aimed at better quantifying the relative contribution of divertor leakage and radial ion transport on neutral pressures surrounding the core are described. We find that cross-field transport competes with, or dominates, parallel transport in such a way that plasma exists far out in the SOL shadow, thus leading to recycling. Changing the core transport from L- to H-mode leads to little or no effect on the far SOL indicating that the flux to the walls has not changed, just the gradients at the separatrix and the density in the core.

The recycling in the main chamber due to cross-field transport appears to be an important source for neutrals for lower divertor operation. Estimates of the contribution of lower divertor leakage to the midplane pressure range from 10-30%. At this time we do not know whether the relative contributions to the main chamber pressure by main chamber recycling and lower divertor leakage vary with operating conditions. The leakage out of the upper divertor is much higher than from the lower divertor. Even so, we find its contribution to the midplane pressure to be similar to that of main chamber recycling.

The results presented lead us to suspect two possible reductions in neutral fluxes before they reach the midplane: 1) the flux out of the divertor itself (based on areas and pressures measured in a port) are lower than a simple, free molecular flow estimate; and 2) neutrals traveling towards the midplane are being redirected away from the midplane through ionization, charge-exchange or elastic scattering. The latter attenuation would explain the observed toroidal and poloidal e-folding lengths for the escaping neutrals of ~ 50 and 20 cm respectively. The importance of

neutral leakage might be significantly altered if the location where neutrals escape into the main chamber were located farther from the plasma, allowing easier passage around the plasma.

The open divertor can compete with the more closed lower divertor in compressing neutrals in the divertor. But in other aspects it fails to be competitive - minimization of neutral leakage and the geometrical aspects of heat reduction.

Acknowledgements – The authors would like to thank C. Boswell and S. Wolfe for invaluable assistance in the second separatrix scan studies. We also thank J. Goetz, P. Stangeby, J. Terry and D. Whyte for many stimulating discussions. This work supported by the U.S. Department of Energy under Grant No. DE-FC02-99ER54512.

References

- [1] Umansky M. V., Krasheninnikov S. I., LaBombard B., and Terry J. L. 1998 *Physics of Plasmas* **5** 3373
- [2] Umansky M. V., Krasheninnikov S. I., and LaBombard B. 1999 *Physics of Plasmas* **6** 2791
- [3] Labombard B., Lipschultz B., Goetz J. *et al*, "Cross-field transport in the SOL: Its relationship to main chamber and divertor neutral control in Alcator C-Mod," in *Plasma Physics and Controlled Fusion Research* (IAEA, Vienna (2001), Sorrento, 2000).
- [4] LaBombard B., Umansky M. V., Boivin R. L. *et al* 2000 *Nuclear Fusion* **40** 2041
- [5] LaBombard B., Boivin R. L., Greenwald M. *et al* 2001 *Physics of Plasmas* **8** 2107
- [6] Bosch H. S., Neuhauser J., Schneider R. *et al* 1995 *Journal of Nuclear Materials* **220-220** 558
- [7] Ulrickson M. and Post D. E. 1983 *Journal of Vacuum Science & Technology A-Vacuum Surfaces & Films* **1** 907
- [8] McCormick K., Fiedler S., Kyriakakis G., Neuhauser J., Reiter D., Schneider R., Schweinzer J., and N. Tsois N., "Particle and Energy Transport in the ASDEX Scrape-Off Layer," in *Controlled Fusion and Plasma Physics* (European Physical Society, Geneva (1993), Lissabon, 1993), Vol. 2, pp. 597.
- [9] Asakura N., Koide Y., Itami K., Hosogane N., Shimizu K., Tsuji-Iio S., Sakurai S., and Sakasai A. 1997 *Journal of Nuclear Materials* **241-243** 559
- [10] LaBombard B., Goetz J. A., Hutchinson I. *et al* 1997 *Journal of Nuclear Materials* **241-243** 149
- [11] Shimizu K., Itami K., Kubo H., Asakura N., and Shimada M. 1992 *Journal of Nuclear Materials* **196-198** 476
- [12] Owen L., Carreras B., Mioduszewski P., Boivin R. L., Hubbard A. E., LaBombard B., Pitcher C. S., and Terry J. L. 1998 *Bull. Amer. Phys. Soc.* **43** 1823
- [13] Pitcher C. S., Boswell C. J., Goetz J. A., LaBombard B., Lipschultz B., Rice J. E., and Terry J. L. 2000 *Physics of Plasmas* **7** 1894
- [14] Loarte A. 2001 *Plasma Physics & Controlled Fusion* **43**
- [15] Stangeby P. C. 1984 *Journal of Nuclear Materials* **121** 55
- [16] Horton L. D., Vlases G. C., Andrew P. *et al* 1999 *Nuclear Fusion* **39** 1
- [17] Kawashima H., Sengoku S., Ogawa T., Ogawa H., Uehara K., Miura Y., and Kimura H. 1999 *Nuclear Fusion* **39** 1679
- [18] Allen S. L., Brooks N. H., Bastasz R. *et al* 1999 *Nuclear Fusion* **39** 2015
- [19] Monk R. D. 1999 *Nuclear Fusion* **39** 1751
- [20] Bosch H. S., Ullrich W., Bard A., Coster D., Haas G., Kallenbach A., Neuhauser J., and Schneider R. 1999 *Journal of Nuclear Materials* **266-269** 462
- [21] Schneider R., Bosch H. S., Coster D. *et al* 1999 *Journal of Nuclear Materials* **266-269** 175

- [22] Pitcher C. S., LaBombard B., Danforth R., Pina W., Silveira M., and Parkin B. 2001 *Review of Scientific Instruments* **72** 1
- [23] Lao L. L., St. John H. , Stambaugh R. D., Kellman A.G., Pfeiffer W., and 1611 Nucl. Fusion 25 (1985) 1985 *Nuclear Fusion* **25** 1611
- [24] Boivin R. L., Goetz J. A., Hubbard A. E. *et al* 2000 *Physics of Plasmas* **7** 1919
- [25] Carreras B., Lynch V.E., and LaBombard B. 2001 *Physics of Plasmas* **8** 3702
- [26] Terry J. L., Maqueda R., Pitcher C. S., Zweben S. J., LaBombard B., Marmor E. S., Pigarov AYu, and Wurden G. 2001 *Journal of Nuclear Materials* **290** 757
- [27] Pitcher C. S., Erents S.K., Fundamenski W. *et al* 2001 *Proc. of the 28th Eur. Physical Society Conf. on Controlled Fusion and Plasma Physics* (Madeira, Portugal, 18-22 June 2001) NA
- [28] Nachtrieb R. and LaBombard B. 2000 *Physics of Plasmas* **7** 4573
- [29] McCracken G. M., Lipschultz B., Labombard B. *et al* 1997 *Physics of Plasmas* **4** 1681
- [30] Lipschultz B., Pappas D. A., LaBombard B., Rice J. E., Smith D., and Wukitch S. J. 2001 *Nuclear Fusion* **41** 585
- [31] Niemczewski A., Hutchinson I. H., LaBombard B., Lipschultz B., and McCracken G. M. 1997 *Nuclear Fusion* **37** 151

Figure captions:

Figure 1: Poloidal (a) and toroidal cross-section of Alcator C-Mod the lower closed divertor and open upper divertor. Baratron capacitance manometer pressure gauges are located in the vertical ports at locations 1,9 and 10. A shielded Bayard-Alpert gauge is at location 5 in a horizontal port. Penning gauges are attached the wall of the vessel at locations 3 & 6. Scanning probes are inserted horizontally (4) and vertically (7). Divertor bypass valves are located at 10 points poloidally (8). Two thin ($\sim 1\text{cm}$ toroidal extent) plates/gussets are located on either side of each of 10 vertical ports with protection tiles on each edge (2).

Figure 2: SOL parameters and the effect of increasing \bar{n}_e . a) n_e profiles; b) T_e profiles; c) scaling of the inferred radial ion flux density at the limiter radius, $\Gamma_{\perp,\text{lim}}$, vs. midplane pressure (lower axis) and equivalent radial influx of neutrals (upper axis).

Figure 3: Effect of transition from L- (open circles) to H-mode (closed circles) on the SOL. a) n_e profile; b) T_e profile; c) v_{\perp} profile; and d) $v_{\perp,\text{min}} \sim Mc_s \lambda_{\perp} / L$. The location of the limiter is given by the vertical shaded region.

Figure 4: Scaling of the density at the limiter radius, $n_{e,\text{lim}}$ (a), $\Gamma_{\perp,\text{lim}}$ (b), and midplane pressure (c, location 5 in Figure 1) vs. \bar{n}_e . L-mode (open circles) and H-mode (closed circles) are shown. The H-mode discharges have the same far SOL parameters as the L-mode discharges from which they arose.

Figure 5: The effect of shifting a diverted discharge against the inner wall. The gaps between the separatrix and the inner wall and outer limiters are given in the figure.

Figure 6: Scaling of outer wall (midplane) pressure vs. various divertor pressures during lower x-point, 800 kA, L-mode discharges. a) Lower divertor (closed); b) lower divertor (open port); and c) open upper divertor. Detached plasmas are shown as filled symbols. Fits to the various data sets are shown as lines.

Figure 7: Effect of limiting the plasma on the divertor and outer wall (midplane) pressures. The data are from the same discharges as Fig. 5.

Figure 8: Utilization of the first to second separatrix gap (SSEP) to change the divertor pressures and the resultant effect on the outer wall (midplane) pressure. SSEP is varied from discharge to

discharge. L- and H-mode cases are included. The divertor pressures have been fit (lines through data) and the used as input to the model of Eq. 6 with the resultant prediction of the midplane pressure (line through data).

Figure 9: The effect of an SSEP scan in one shot from single null at the lower divertor ($SSEP < 0$) to single-null at the upper divertor ($SSEP > 0$) is given by the solid line. A reference case with the standard single-null at the lower divertor is also shown (dashed line).

Figure 10: Three divertor bypass valves (toroidal locations -18° , $+18^\circ$, $+54^\circ$) are opened and closed with ~ 200 ms full period. The period when the bypass valves are opened or closed is shaded and marked in b). The relative toroidal locations of the valves and gauges are given in Fig. 1b).

Figure 11: Summary of the results from discharges where the toroidal location of the 3 bypass valves is varied. The data are divided into two cases – bypass valves opened near the outer wall (lower) gauge (solid lines and circles) and far from that gauge (dashed lines and triangles). a) change in \bar{n}_e vs. time; b) change in outer wall (lower) pressure vs. time; c) change in outer wall (lower) pressure vs. change in \bar{n}_e ; and d) change in outer wall (lower) pressure vs. change in \bar{n}_e .

Figure 1

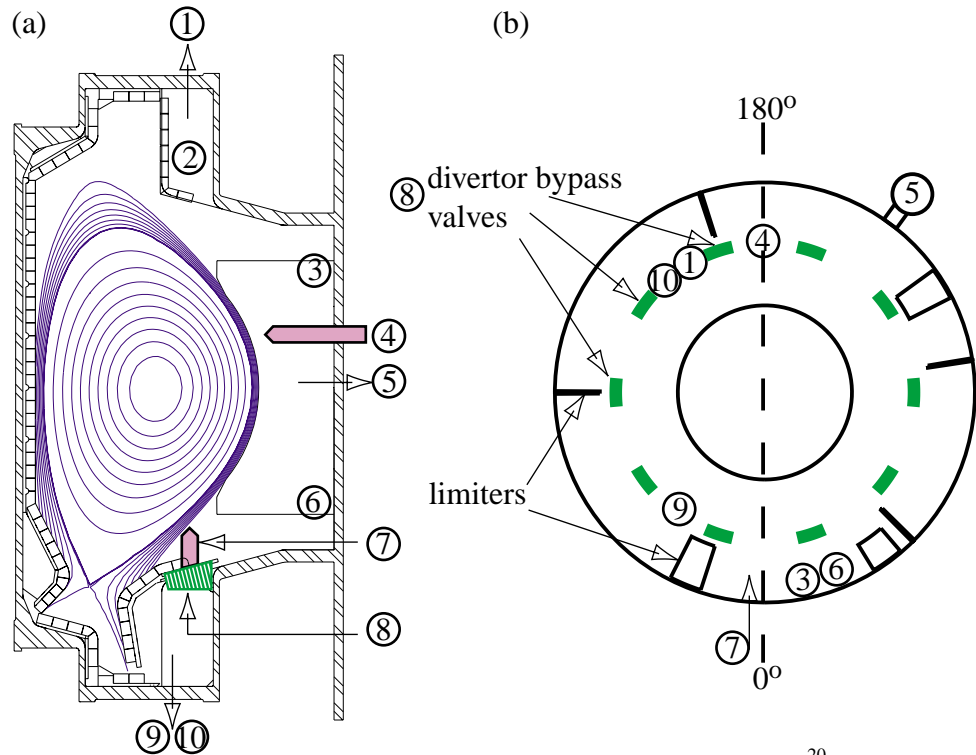


Figure 2

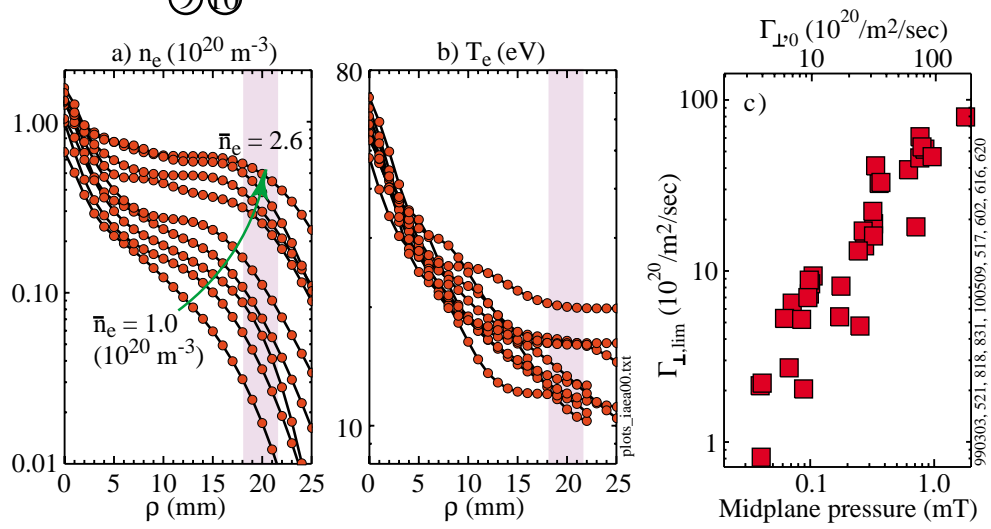


Figure 3

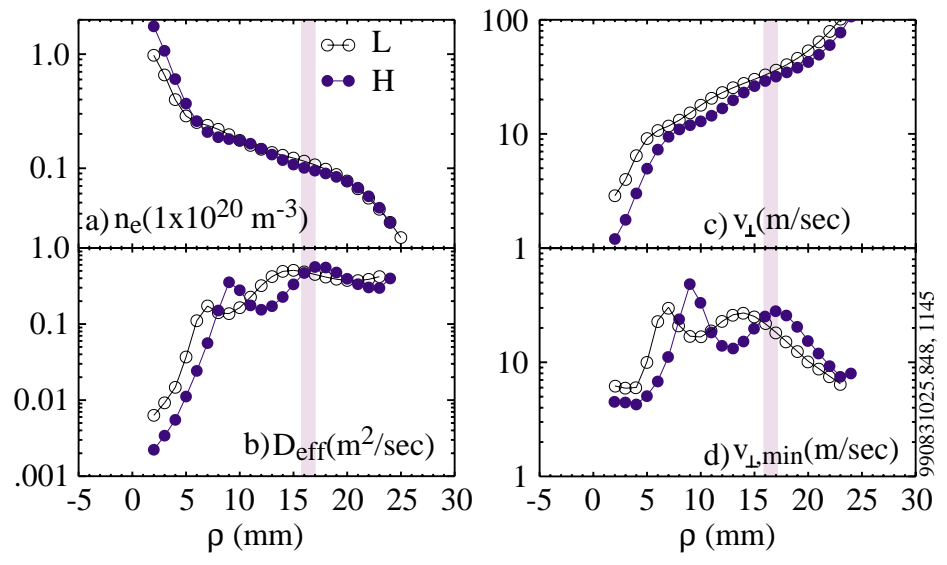


Figure 4

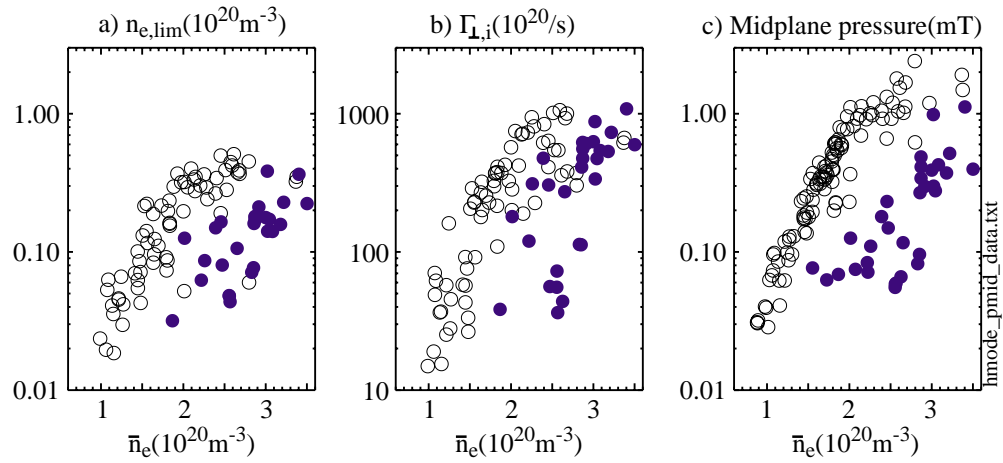


Figure 5

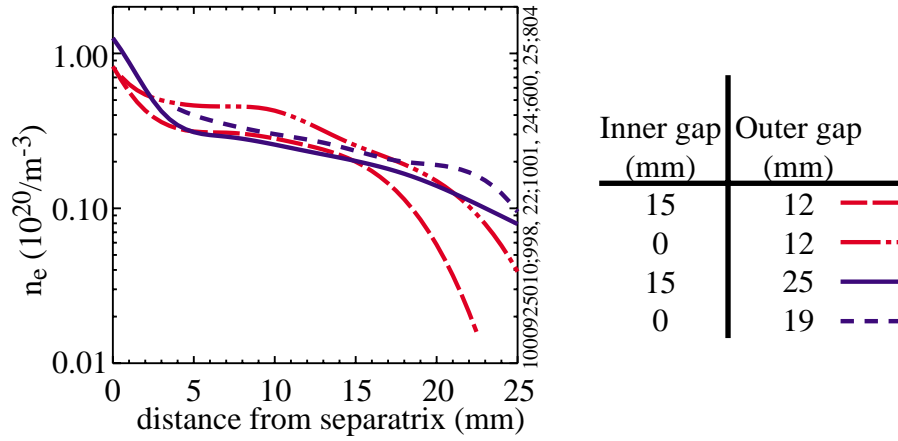


Figure 6

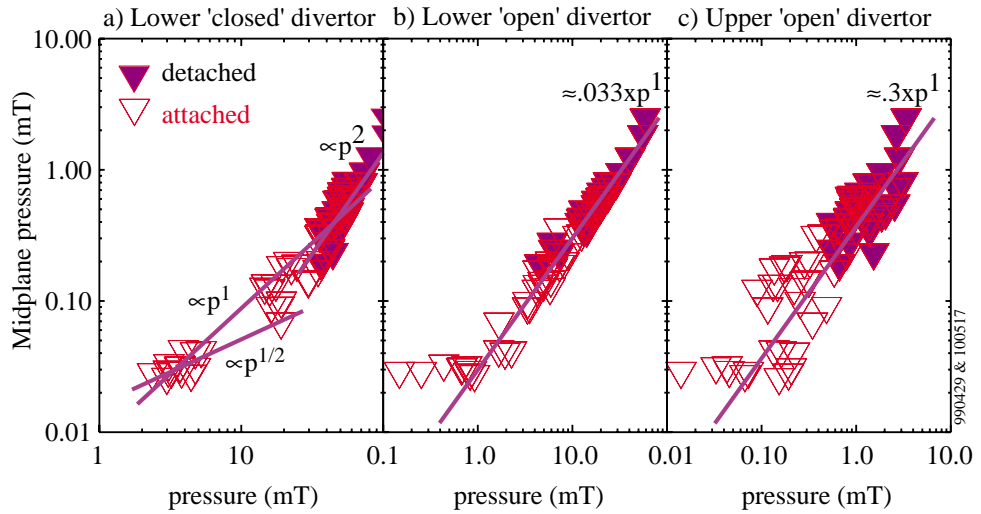


Figure 7

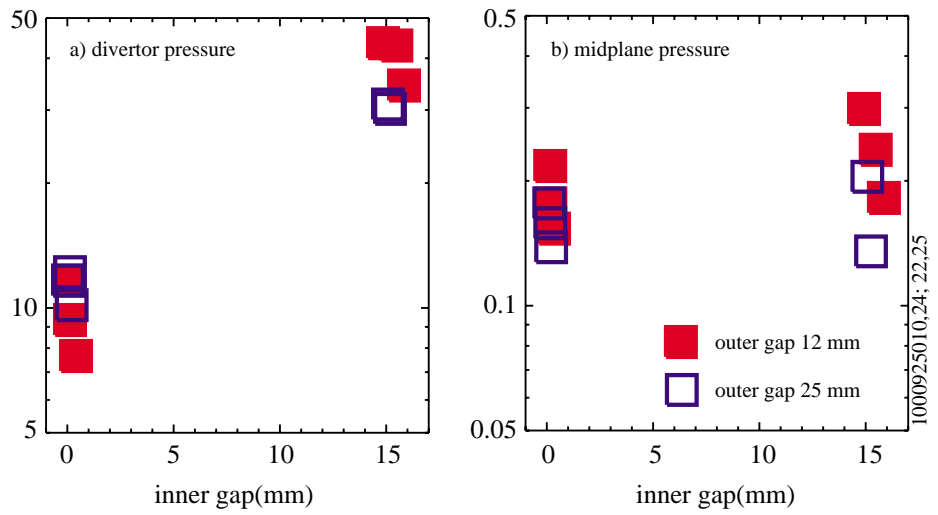


Figure 8

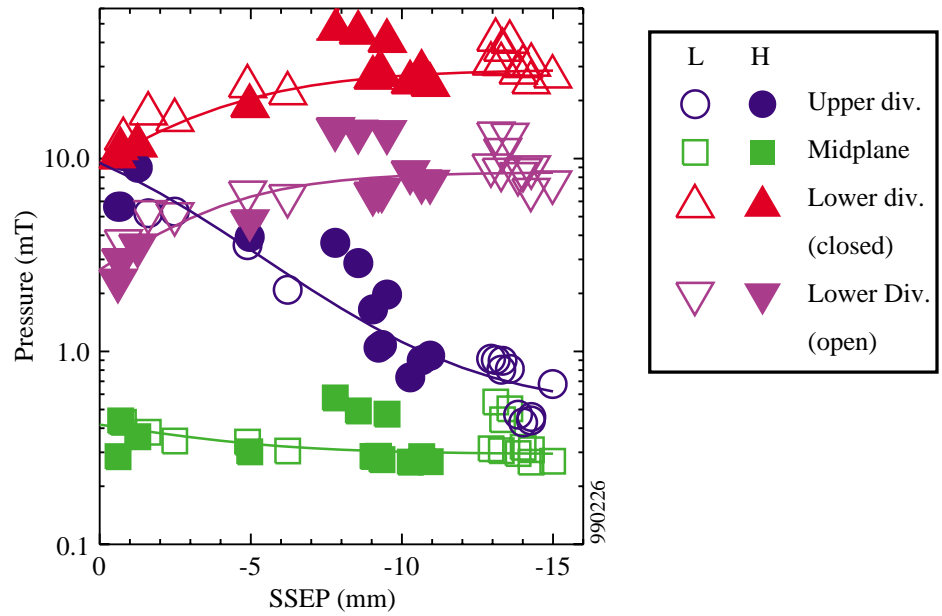


Figure 9

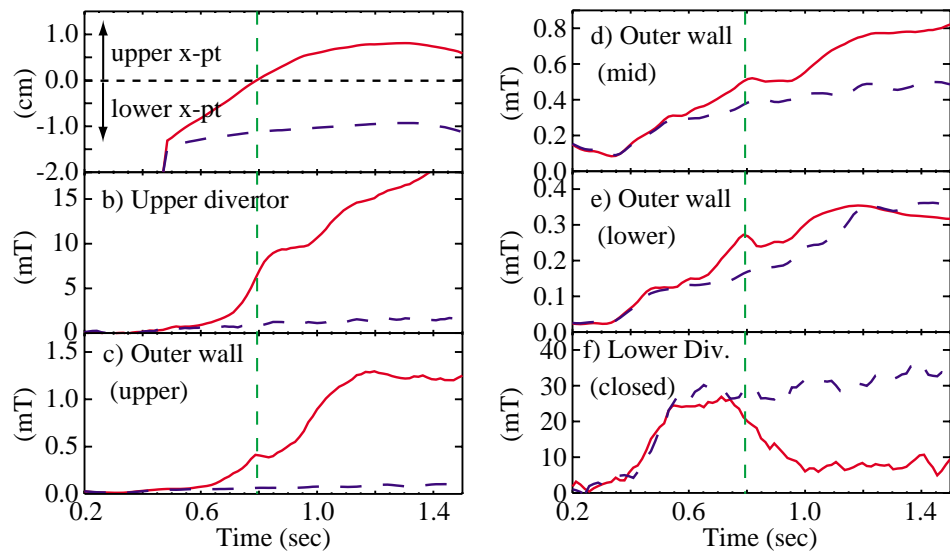


Figure 10

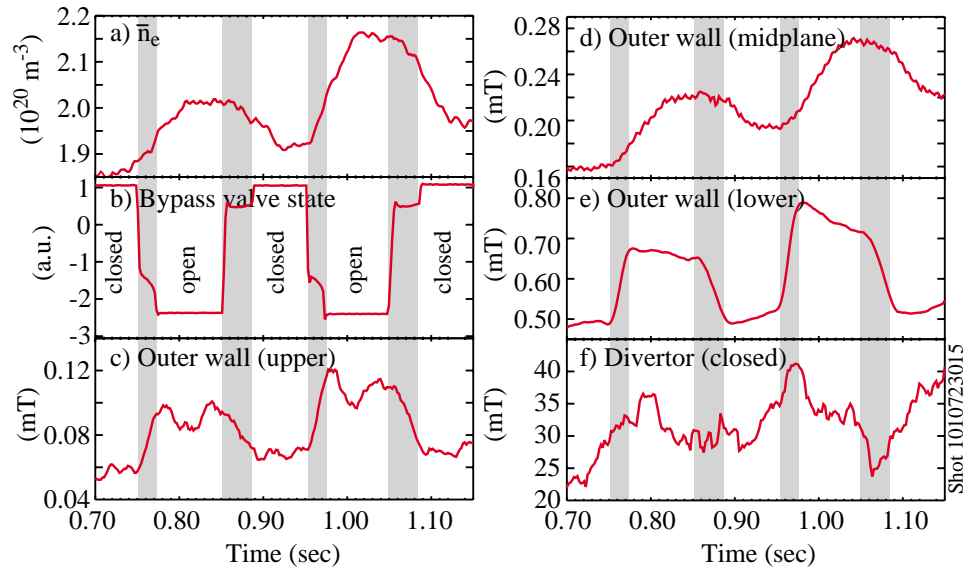


Figure 11

